Thesis

Arm Length Compensation System for Underground Gravitational-wave Telescope

Koseki Miyo

Department of Physics
University of Tokyo

MMM 2020

Contents

Chapter 1

Background

1.1 Gravitational-wave

1.2 Sources of gravitational-wave

1.3 Interferometric Gravitational-wave detection

1.4 Terrestrial Laser Interferometers

1.5 KAGRA

1.6 Summary of the Chapter

Chapter 2

Geophysics Interferometer (GIF)

2.1 Overview

2.2 Purpose

2.2.1 Motivation in Geophysics

2.2.2 Motivation in GW detectors

2.3 Working Principle

2.3.1 Asynmetric Michelson Interferometer

$$\phi = 2\pi \frac{2(l_x - l_y)}{\lambda} \sim 4\pi \frac{l_x}{\lambda} \tag{2.1}$$

$$|d\phi| = 4\pi \frac{l_x}{\lambda} \left(\left| \frac{d\lambda}{\lambda} \right| + \left| \frac{dl_x}{l_x} \right| \right) \tag{2.2}$$

2.3.2 Response to the seismic strain

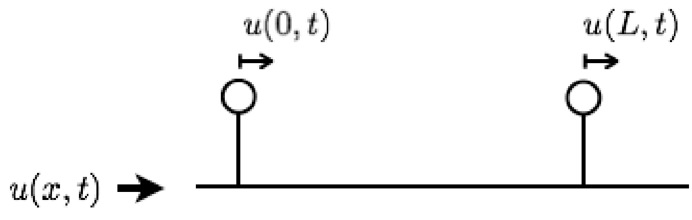

Figure 2.1: The displacements of the two points which are sparated L in X axis.

The response of the strainmeter to seismic waves have characteristics of the low pass filter. To calculate this response, it is assumed that the plane seismic waves which displacement $u(x,t)$ is represented as $u(x,t) = u_0 e^{i(\omega t - kx)}$ with angular frequency of ω and wave number of k, propagate along with the direction of the base-line of the strainmeter. The length fluctuation between two mirrors sparated with L can be expressed as

$$\Delta L(t) \equiv u(0,t) - u(L,t) \tag{2.3}$$
$$= u(0,t) - u(0,t-\tau), \tag{2.4}$$

where $\tau = L/v$ is the time delay. The transfer function from the displacement to the length fluctuation is

$$H_{\mathrm{disp}}(s) \equiv \frac{\Delta L(s)}{u(s)} = 1 - \exp(-\tau s) \tag{2.5}$$

Because the strain amplitude $\epsilon(x,t)$ is defined as $\epsilon(x,t) \equiv \frac{du}{dx}$, the strain

$$\epsilon(x,t) \equiv \frac{du}{dx} = \frac{du}{dt}\frac{dt}{dx} \tag{2.6}$$
$$= u(x,t)' \frac{1}{v} \tag{2.7}$$

Therefore, the response of the strainmter to the seismic strain is given

$$H_{\mathrm{strain}}(s) \equiv \frac{\Delta L(s)}{\epsilon(s)} = \frac{\Delta L(s)}{\frac{s}{v} u(s)} = (1 - \exp(-\tau s))\,\frac{v}{s} \tag{2.8}$$

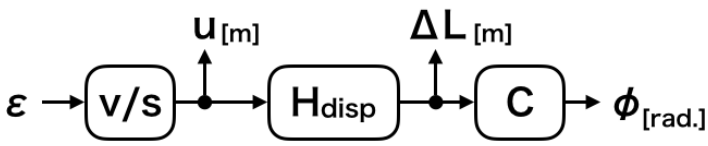

Figure 2.2

2.3.3 Signal Detection Scheme

Quadrature Phase Detection

2.3.4 Noise

どういうノイズが原理的に存在するか述べる。空気ゆらぎ、周波数雑音を述べる。

2.4 Optics

どうやって実際の干渉計を構築しているか述べる。

2.4.1 Mode Matching Optics

どういうモードマッチをして干渉計として光を干渉させているか述べる。

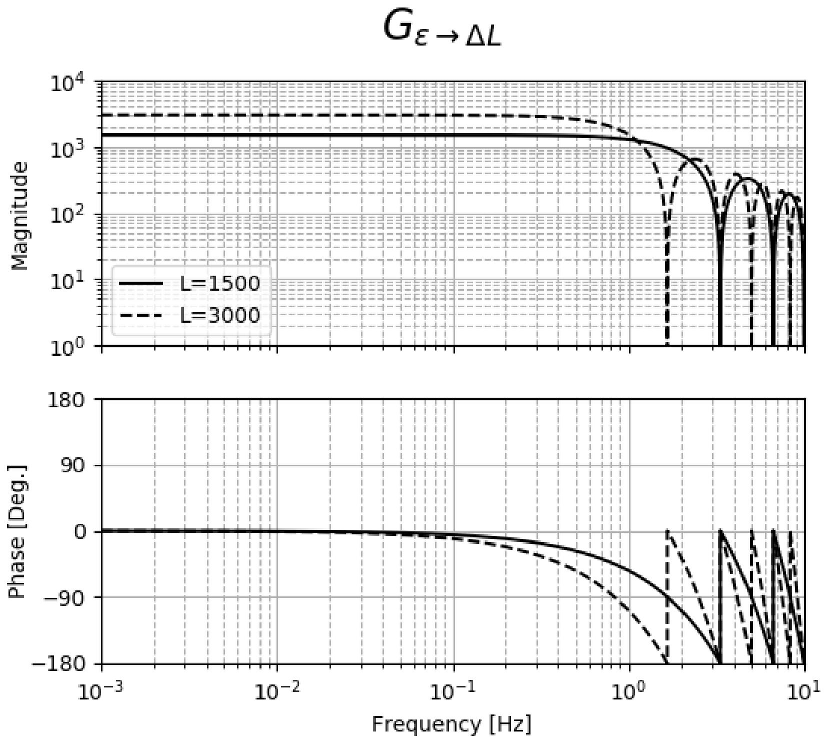

Figure 2.3

2.4.2 Frequency Stabilized Laser

どういう制御をして周波数安定をしているか述べる。

2.4.3 Core Optics

Beam Splitter

どういうミラーを使っているか述べる。

Corner Cube

どういうミラーを使っているか述べる。大きさとか表面の精度とか。

2.5 Data Aquisition System

DAQ について述べる。冗長性を持たせるために二系統の DAQ を使っていることを述べる。一方は KAGRA とは独立で、もう一方は KAGRA と同じシステムに組み込んでいることを述べる。

2.5.1 Stand Alone System

森井システムについてのべる。コンパクトなシステムで地下環境でも安定して動くシステムだ、と述べる。

2.5.2 Realtime System

KAGRA のリアルタイムシステムについて述べる。KAGRA の制御に組み込むために歪変換をリアルタイムで行っている、と述べる。

2.6 Summary of the Chapter

本章で述べたパラメータを表にまとめる。

Chapter 3

Seismic Noise Under the Ground

3.1 Introduction

3.1.1 Surface Site

3.1.2 Underground Site

3.1.3 KAGRA Site

3.2 Theory of Seismic Waves

3.2.1 Seismic Waves

3.2.2 Depth Dependence

3.2.3 ...

3.3 Seismic Noise

3.3.1 Problematic Seismic Noise

3.3.2 Microseisms

3.3.3 Earthquakes

(Write how earthquakes disturb the large scale interferometer.)

Mechanism

遠方での大きな地震は脈動帯域以下の低周波地面振動を励起し、ロックロスの原因になる。

Early Earthquake Alert

Seismon をつかって到来時間を予測し、この低周波地面振動の RMS を抑えるための特別なフィルターに切り替えて、ロックロスをへらす工夫を行っている。しかし、このフィルターは脈動がうるさいときは再びロックロスの問題を抱えてしまう。

3.3.4 Earth Tides

3.3.5 ...

3.4 Differential Motion Reduction

3.4.1 Introduction

The motion of two mirrors in the cavity have two modes. One is differential motion, which is the length change of that. Another one is common motion, which is the motion of the center of the cavity. In terms of the length control, it is important that the RMS amplitude of differential motion is as small as possible. Actuarlly, the amplitude of these two motions are the same each other when the mirrors moves with no coherence. However, when a coherence exists, the common motion tends to be larger than the differential one.

As discussed in this section, the coherence depends on both, the arm length and the wavelength of seismic waves. For example, if the arm length is much more smaller than the wavelength, the mirrors move together. This means that the common motion is greater than the differential motion.

The ratio of the amplitudes of the differential motion over common motion is newly defined as Common and Differential Motion Ratio (CDMR). It is usefull to know how the ground reducts the differential motion or increase the common motion.

3.4.2 Differential Motion Reduction

Differential Motion and Common Motion

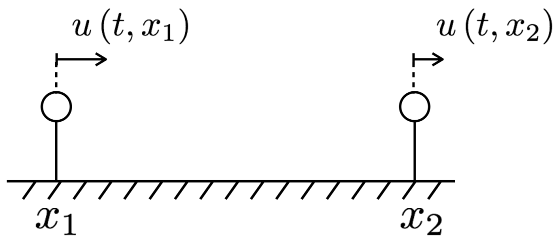

Figure 3.1: Displacements of the two points; x_1 and x_2. Displacements of each point are represented as $u(x_1, t)$, $u(x_2, t)$, where $u(x, t)$ is the displacement of the seismic wave.

Motions of the two points can be represented as the differential motion and the common motion. Displacement of both differential motion and common motion of the two points shown in Figure(3.1) are defined as

$$u_{\text{diff}} \equiv \frac{u_1 - u_2}{\sqrt{2}},\ u_{\text{comm}} \equiv \frac{u_1 + u_2}{\sqrt{2}} \tag{3.1}$$

where $u_1(x, t)$ and $u_2(x, t)$ are the displacement of each points. These two motions defined in Eq.(3.1) are normalized by $\sqrt{2}$ due to conserve the total power.

Common and Differential Motion Ratio (CDMR)

CDMR is defined as the powers of common motion over the differential motion as bellow,

$$\mathrm{CDMR} \equiv \sqrt{\frac{\text{Common Motion}}{\text{Differential Motion}}} = \sqrt{\frac{P_{\mathrm{comm}}(\omega)}{P_{\mathrm{diff}}(\omega)}} \tag{3.2}$$

where $P_{\mathrm{comm}}, P_{\mathrm{diff}}$ are the power spectral densities (PSDs) of the differential motion and common motion, respectively. Each PSDs are converted from the autocorrelation function of these by the Wiener-Khinchin theorem.

First, autocorrelation function C_{diff} of the differential motion is given by its definition in Eq.(3.1)

$$C_{\mathrm{diff}}(\tau) = \frac{1}{2}\left\langle \left[x_1(t) - x_2(t)\right]\left[x_1(t+\tau) - x_2(t+\tau)\right]\right\rangle \tag{3.3}$$

$$= \frac{1}{2}\left[C_{11}(\tau) - C_{12}(\tau) - C_{21}(\tau) + C_{22}(\tau)\right], \tag{3.4}$$

,where C_{ij} are the autocorrelation functions of each point and defined as $C_{ij} \equiv \langle x_i(t)x_j(t+\tau)\rangle$, $(i = 1, 2,\ j = 1, 2)$. Therefore, the power spectrum density of differential motion $P_{\mathrm{diff}}(\omega)$ can be computed as

$$P_{\mathrm{diff}}(\omega) = \frac{1}{2}\left[P_1(\omega) + P_2(\omega) - P_{12}(\omega) - P_{12}^*(\omega)\right] \tag{3.5}$$

$$= \frac{1}{2}\left[P_1 + P_2 - \mathrm{Re}\,[\gamma] \times 2\sqrt{P_1 P_2}\right] \tag{3.6}$$

where $P_1(\omega), P_2(\omega)$ are the power spectrum densities of each points, and $P_{12}(\omega)$ are the cross spectrum between two point. The parameter γ is the complex coherence between them defined below,

$$\gamma \equiv \frac{P_{12}}{\sqrt{P_1 P_2}}. \tag{3.7}$$

Here, assuming that seismic wave propagating each points does not decay, which means $P_1 = P_2 \equiv P$, one can compute the $P_{\mathrm{diff}}(\omega)$ as

$$P_{\mathrm{diff}}(\omega) = P(1 - \mathrm{Re}\,[\gamma]). \tag{3.8}$$

Therefore, the PSDs of the common motion can be calculated as

$$P_{\mathrm{comm}}(\omega) = P(1 + \mathrm{Re}\,[\gamma]). \tag{3.9}$$

Finaly, CDMR defined Eq.(3.2) in case the seismic wave does not decay is represented as

$$\mathrm{CDMR} = \sqrt{\frac{1 + \mathrm{Re}\,[\gamma]}{1 - \mathrm{Re}\,[\gamma]}}\,. \tag{3.10}$$

Eq.(3.10) indicate that CDMR can be expressed by only the coherence γ between of two points. For example, CDMR tends to be larger when γ close to 1. This means that the differential motion is more less than the common motion because the two points move together in the same direction.

CDMR of the X-arm Ground

3.5 Summary of the Chapter

Chapter 4

KAGRA Interferometer

4.1 Overview

4.1.1

4.1.2

4.2 Main Interferometer

4.2.1

4.2.2

4.3 Vibration Isolation

4.3.1

4.3.2

4.4 Summary of the Chapter

Chapter 5

Demonstration of Arm Length Compensation Control

5.1 Control Design

5.1.1

5.1.2

5.1.3

5.2 Experimental Arrangement

5.2.1

5.2.2

5.2.3

5.3 Result

5.3.1

5.3.2

5.3.3

5.4 Summary of the Chapter

Chapter 6

Conculusion and Future Directions

6.1 Conclusion

6.2 Future Directions